A 600 W 6.78 MHz Wireless Charger for an Electric Scooter

Christopher H. Kwan, Juan M. Arteaga, Samer Aldhaher, David C. Yates and Paul D. Mitcheson
Department of Electrical and Electronic Engineering
Imperial College London
London, United Kingdom
christopher.kwan@imperial.ac.uk

***Abstract*—This paper presents a 600 W electric scooter wireless charging solution operating at a frequency of 6.78 MHz. At the transmitter end, a load-independent Class EF push-pull (differential) inverter with GaN transistors was used to drive a 33 cm square-shaped copper pipe coil. A full-wave voltage-tripler Class D rectifier with silicon Schottky diodes was connected to a 24 cm-by-26 cm trapezoidal receiver coil (also made of copper pipe) mounted underneath the steel frame of the scooter. In order to reduce the eddy current and magnetic losses in the steel chassis, parts of the electric scooter frame were shielded with copper tape. With the battery recharging in situ at 600 W, the IPT system achieved a DC-to-DC efficiency of 84 %.**

***Index Terms*—Inductive power transmission, inductive charging, electric vehicles**

I. Introduction

In recent years, many cities around the world have seen a rapid increase in the popularity of light-weight e-mobility in the form of electric scooters (both kick-scooters and motorcycles with a step-through frame) and electric bicycles. At present, these vehicles are recharged primarily by plugging into the mains via a power cable. In addition, there is a growing number of electric bicycle and motorcycle hire schemes in urban areas, which rely on maintenance staff to swap the batteries of these vehicles that are scattered all over different parts of a city. In both scenarios, it is clear that wireless charging can offer significant benefits, as it removes the direct interaction between the riders and the charging mechanism. This leads to a more convenient, reliable and safer method of recharging the batteries.

This paper focuses on the development of a 6.78 MHz (ISM band) inductive power transfer system for electric scooters (the motorcycle-type); these vehicles have larger batteries than kick-scooters and bicycles, so they need to be charged at high power levels. It describes the design of the IPT coils, magnetic link and the high-frequency power electronics, evaluates the safety of the IPT system with respect to ICNIRP limits on human exposure to electromagnetic fields, and presents experimental results of the complete wireless charger system integrated in the electric scooter. In previous work [1], the authors described the design and construction of a 100 W inductive power transfer system for charging an electric scooter. As will be outlined below, the particular model of electric scooter considered in this work has a battery that charges at a much higher rate of 600 W; therefore, different coil designs and power electronics topologies are required in order to scale up the power, compared with the system in [1].

Fig. 1. GOVECS GO! S2.4+ electric scooter [2]

The electric scooter for which the wireless charger is being designed is the GOVECS GO! S2.4+ (Fig. 1), which has a 72 V 30 A h lithium-ion rechargeable battery that is sitting on the steel frame at the bottom of the scooter. This particular model of electric scooter is supplied with a Mean Well 83.7 V off-board charger that accepts either an AC mains input voltage of 90 V to 246 V or a DC input voltage of 127 V to 370 V, and provides a maximum charging current of 7.2 A to the battery. Hence, the maximum charging rate of the charger is 600 W. This charger has been placed inside the scooter frame with a custom-designed mount in order to convert it into an 'on-board' charger, so that the electric scooter is able to start its battery charging process seamlessly as soon as it is parked over a charging pad.

II. Coil and magnetic link design

The transmitter coil (Fig. 2a) consists of a 2-turn 33 cm square coil made of 10 mm copper pipe, with a spacing of 10 mm between the turns. Electromagnetic simulations performed in CST Microwave Studio show that the inductance of this coil is 2.76 µH and the Q factor is 1685 (the coil has a high Q factor due to the use of copper pipe).

The receiver coil (Fig. 2b) is a 3-turn trapezoidal coil made of 8 mm copper pipe, with a length of 26 cm, a width of 15 cm at the front, a width of 24 cm at the rear, and a spacing

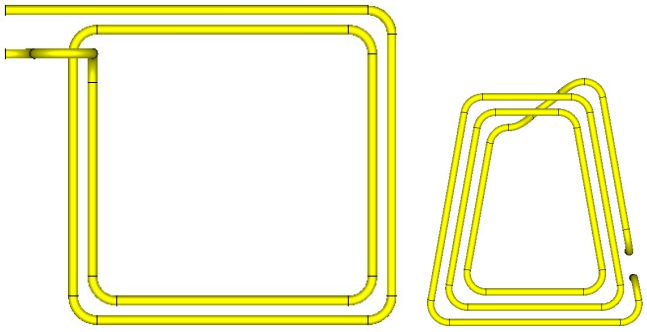

(a) Transmitter coil (b) Receiver coil

Fig. 2. Coils for electric scooter wireless charger

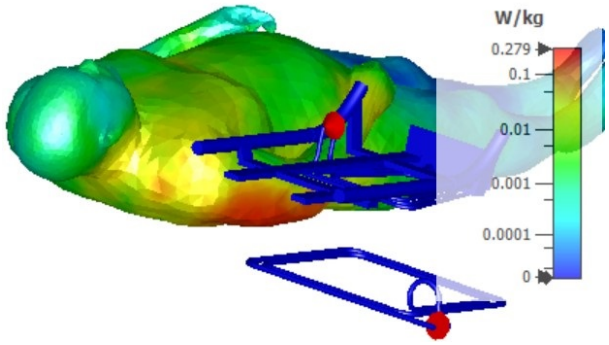

Fig. 3. SAR plot – Nelly lying down

TABLE I
LINK PARAMETERS FOR 600 W

Parameter	Value
k	7.0 %
η_{link}	97 %
I_1	15.10 A
I_2	11.32 A
C_S	267 pF
R_L	9.37 Ω
R_{refl}	5.33 Ω

of 10 mm between the turns. The geometry of the receiver coil was specially designed to fit inside the body panel that covers the underside of the scooter frame. In air, this coil has a simulated inductance of 2.80 µH and a Q factor of 1412.

As the receiver coil is to be mounted fairly close to the scooter's steel frame, its inductance and Q factor will be altered due to steel's conductivity and magnetic permeability. In order to reduce the eddy current losses and magnetic losses in the steel chassis, parts of the steel frame were covered in copper tape as a form of shielding, as copper has a higher conductivity and a relative permeability of 1. Assuming that the shield is at least five skin depths thick, which for copper at 6.78 MHz is $5 \times 25\,\mu\text{m} = 125\,\mu\text{m}$, the scooter frame can be modelled as solid copper in the electromagnetic simulations. Due to the presence of the copper tape-shielded scooter frame, the receiver coil has a simulated inductance of 2.06 µH and a Q factor of 725.

The distance between the transmitter coil and the receiver coil is 17 cm. At this separation distance, the coupling factor in air is 8.9 %. However, the presence of the metal frame and chassis causes the coupling factor to drop to 7 %. Given the in situ coil impedances and coupling factor, the link parameters for 600 W of received power with a series-tuned receiver and the optimal load for achieving maximum link efficiency have been derived and are given in Table I, where k is the coupling factor, η_{link} is the link efficiency, I_1 and I_2 are the primary and secondary coil current amplitudes, C_S is the secondary series tuning capacitance, R_L is the optimal load resistance and R_{refl} is reflected resistance seen at the transmitter end.

A. Human exposure safety

In order to deploy a wireless charging system for electric scooters in publicly-accessible locations, the compliance of such a system to human electromagnetic field exposure limits needs to be evaluated. For human exposure safety, as the frequency of operation is 6.78 MHz, the basic restrictions from ICNIRP 1998 (thermal effects – specific absorption rate) and ICNIRP 2010 (non-thermal effects – internal E-field) are relevant.

Simulations of the 600 W electric scooter wireless charging system with the Nelly human body CAD model were performed in CST Microwave Studio. Fig. 3 shows the SAR plot of Nelly in the lying (supine) position 5 cm from the transmitter coil (coil centre aligned with chest). The maximum localised SAR was 0.28 W kg^{-1} at the right upper arm, which is less than the general public exposure limit of 4 W kg^{-1} for the limbs. In addition, the 99$^{\text{th}}$ percentile internal E-field value is 38 V m^{-1} which is below the general public exposure limit of 915 V m^{-1}.

III. LOAD-INDEPENDENT CONSTANT-CURRENT PUSH-PULL CLASS EF INVERTER

The concept of load-independent operation was first introduced in [3], which allows Class E inverters to maintain efficient operation by operating constantly at zero-voltage switching (ZVS) and simultaneously achieve either an output voltage or current that is constant in amplitude and phase regardless of the load value and without feedback, tuning, frequency or duty cycle control. The concept of load-independent operation was extended to Class EF inverters and rectifiers in [4] which as a result has enabled the efficient operation of inductive wireless power transfer systems with variable position between transmitter and receiver and variable loading as demonstrated recently in [5].

Fig. 4 shows the circuit diagram of the proposed current-mode push-pull load-independent Class EF inverter. The single-ended configuration of this topology has been thoroughly analysed and full design equations have been derived in [4]. Unlike conventional Class EF$_{\text{n}}$ inverters, here the EF network (L_2 and C_2 in Fig. 4) is not tuned to an integer multiple of the switching frequency, but rather to 1.4-1.8

times the switching frequency. This results in a different set of design solutions that can achieve constant current-mode and ZVS operation over varying loads. The disadvantage of this approach is that the EF branch no longer presents a low impedance to the second or third harmonic, therefore additional filters may be required at the output stage.

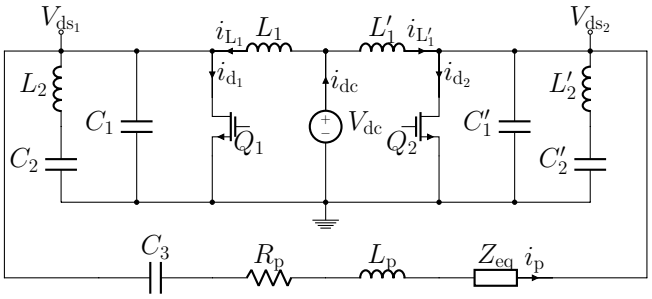

Fig. 4. Push-Pull Class EF inverter circuit topology

The following design equations can be used to design a inverter that operates at the maximum power-output capability case as described in [4]:

$$\frac{1}{\omega\sqrt{L_2C_2}} = q_1 = 1.66 \tag{1a}$$

$$\frac{C_1}{C_2} = 1.2706 \tag{1b}$$

$$\omega R_L C_1 = 0.1182 \tag{1c}$$

$$\omega X C_1 = 0.3403 \tag{1d}$$

$$\frac{I_m R_L}{V_{\text{in}}} = 0.2938 \tag{1e}$$

$$P_o \frac{R_L}{V_{\text{in}}^2} = 0.0432 \tag{1f}$$

It should be noted that the above design equations are for the single-ended Class EF inverter – the outputs of these equations are adjusted for the push-pull configuration by doubling the values of capacitors C_1 and C_2 and halving the value of L_2.

A. Design and construction

Here, we will describe the design and construction process of a 6.78 MHz push-pull load-independent Class EF inverter for the 600 W electric scooter wireless charging system. The DC input voltage is 240 V and the current in the TX coil is required to be up to 18 A, to take into account the losses in the real system. The maximum reflected resistance of the wireless power link is expected to be around 5.5 Ω. Referring to analysis and design equations in [4], load-independent Class EF circuit can be configured to operate at several special cases. Here, we choose to operate at the maximum power-output capability case using the design equations in (1).

Fig. 5 shows a photograph of the built push-pull load-independent Class EF inverter which consists of several modules and boards. The modules, as shown in Fig. 5, are: 1) the main board module which contains input power connectors, filter capacitors, DC chokes and current limiting and protection circuitry. It is implemented on a 4 layer 1.6 mm thick 1 oz copper FR4 PCB. 2) The second module contains the GaN transistors, the gate drivers, resonant capacitors and inductors. It is implemented on an aluminium-core PCB for enhanced thermal performance; heat sinks are attached to back of the board. The GS66508B devices from GaN Systems are used here. 3) The third module interfaces the transmitting coil to the rest of the modules; it contains the series resonant capacitors to tune the transmitting coil and cut-outs to install current sensors. The module is implemented on a 2 layer 1.6 mm 2 oz copper FR4 board. 4) the final module contains the signal generation and duty cycle adjustment circuitry.

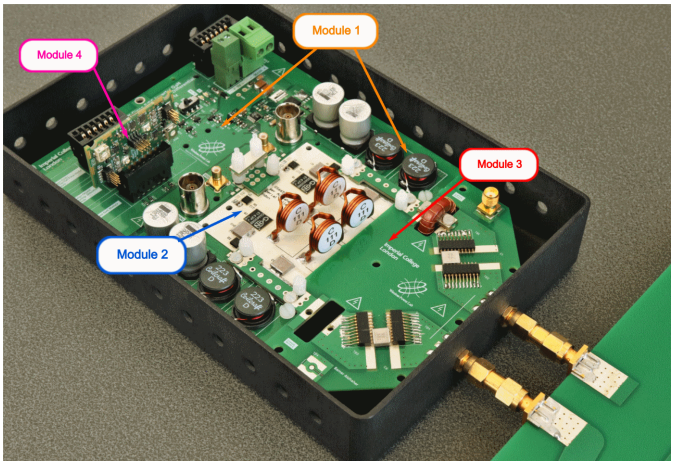

Fig. 5. Photograph of load-independent push-pull Class EF inverter implementation. The inverter consist of 4 modular boards. The GaN FETs and their gate drivers as well the capacitors and inductors are mounted a single-layer aluminium-core PCB for enhanced thermal performance

TABLE II
COMPONENT VALUES AND PARTS USED IN PUSH-PULL LOAD INDEPENDENT CLASS EF INVERTER

Parameter	Value/Implementation
C_1, C_1'	300 pF Vishay QUAD HIFREQ
C_2, C_2'	200 pF Vishay QUAD HIFREQ
C_3, C_3'	730 pF Vishay QUAD HIFREQ
L_1, L_1'	88 µH Coilcraft DO5010H
L_2, L_2'	357 nH Coilcraft 2014VS
L_p	2.54 µH 10 mm copper pipe
Q_1, Q_2	GaN Systems GS66508B
Gate drivers	TI UCC27512DRSR

Table II shows the implemented component values and parts used in the push-pull load-independent Class EF inverter. Due to nonlinear output capacitance of the GaN transistors and the large parasitic capacitances of the aluminium-core PCB, the implemented values of C_1 and C_2 are smaller than the designed or theoretical values.

IV. Full-wave Voltage Tripler Class D Rectifier

A three-stage voltage-multiplier full-wave Class D rectifier has been designed for IPT systems requiring a high output voltage. Fig. 6 shows the circuit schematic of this rectifier,

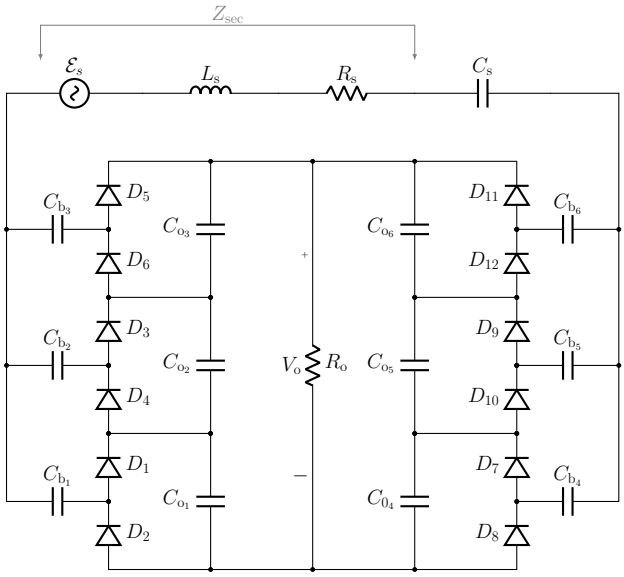

Fig. 6. A voltage-tripler full-wave Class D rectifier for high output voltage.

where C_{s} is designed to resonate with the receive coil and C_{b} is a DC-blocking capacitance that allows each current-driven Class D rectifier to operate at different voltage offsets. The output capacitances, C_{o}, of the three current-driven Class D rectifiers are connected in series to achieve a higher output voltage than that of a full-wave current-driven Class D rectifier.

When a single DC load is fed with multiple rectifiers, the equivalent load fed by each rectifier is a fraction of the actual DC load. In addition, with respect to the source, all the rectifiers are fed in parallel. Therefore, the voltage multiplier principle can be used as an impedance transformation from its input impedance to its output impedance (R_{sec} to R_{o}), and this is dependent on how the individual rectifiers are placed in the topology. This concept, known as the Cockcroft-Walton Voltage Multiplier [6], [7], can comprise an arbitrary number of stages in order to multiply the output voltage (V_o) by a factor equal to the number of stages.

Fig. 6 shows a rectifier design example using this principle where a voltage multiplier rectifier, consisting of six individual Class D rectifiers (or three full-bridge rectifiers) is implemented. Here, each full-bridge rectifier feeds a load equal to $R_{\text{o}}/3$, in parallel, and therefore its theoretical input impedance can be calculated as:

$$Z_{\text{sec}}\Big|_f = \frac{8R_{\text{o}}}{9\pi^2\eta_{\text{rect}}} - j\left(\frac{1}{2\pi f C_{\text{s}}}\right), \tag{2}$$

where η_{rect} is the rectifier's efficiency, R_o is the output DC load and the imaginary part should resonate with the impedance of the receive coil.

This candidate topology is utilised for high output voltage systems such as the electric scooter wireless charger in this paper, where the manufacturer-supplied battery charger requires a minimum input voltage of 127 V to operate. The designed component values are presented in Table III, and the diodes used for this prototype are 100 V, 8 A Schottky diodes by STMicroelectronics (STPS8H100).

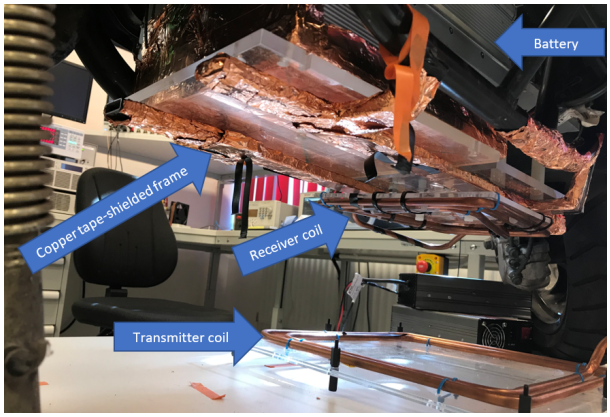

Fig. 7. Scooter charger experimental set-up

TABLE III
COMPONENT VALUES OF THE VOLTAGE-TRIPLER FULL-WAVE CLASS D RECTIFIER

Topology	C_s [pF]	$C_{b_{1-6}}$ [nF]	$C_{o_{1-6}}$ [µF]
3x voltage-multiplier full-wave Class D	268	0.1	1

V. EXPERIMENTAL RESULTS

Fig. 7 shows the experimental set-up of the IPT system in the electric scooter, with the bottom body panel removed to show the position of the mounted receiver coil under the scooter frame, the copper tape-shielded scooter frame and the on-board battery. The transmit coil is driven by the load-independent Class EF inverter, whilst the receive coil is connected to the full-wave voltage tripler Class D rectifier. Whether or not the body panel is in place does not change the IPT link.

Table IV shows the results of the experiment when charging the battery at full power, where V_{dc}, I_{dc} and P_{dc} refer to the DC input voltage, current and power at the inverter end, P_{o} is the power delivered to the equivalent load of the rectifier (i.e. the input power to the manufacturer-supplied battery charger), and $\eta_{\text{dc-load}}$ is the efficiency of the IPT system from the inverter's DC input to the rectifier's equivalent load. Fig. 8 is an oscilloscope trace showing the drain-source voltage waveform of both GaN transistors in the push-pull load independent Class EF inverter – it can be seen that a maximum V_{DS} of 540 V is achieved when a DC input of 240 V is applied.

The distribution of losses of the end-to-end IPT system, derived from simulation and analysis, is as follows: transmitter coil: 14.7 W, receiver coil (including losses in the frame): 10.8 W, inverter loss: 50.1 W, rectifier loss: 37.9 W. A characterisation of the battery charger was performed without the IPT link and an efficiency of 89 % was measured, giving a loss of 67.5 W when charging the battery.

TABLE IV
EXPERIMENTAL RESULTS

Quantity	Value
V_{dc} (V)	240
I_{dc} (A)	3.05
P_{dc} (W)	732
P_{o} (W)	618
$\eta_{\text{dc-load}}$	84.0 %

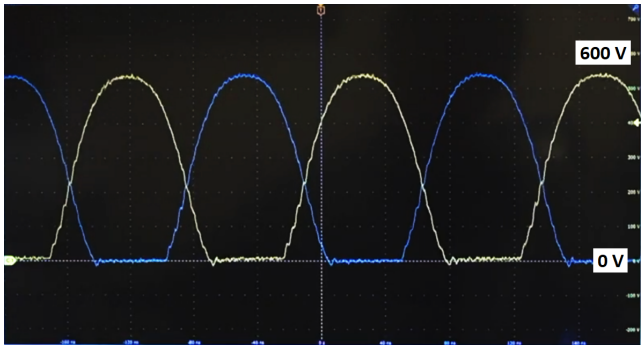

Fig. 8. Scope trace showing V_{DS} waveform of both GaN transistors in push-pull load independent Class EF inverter

VI. CONCLUSION

A 600 W inductive power transfer system has been designed, constructed and integrated into an electric scooter for charging its battery wirelessly. With the use of copper pipe coils, copper tape shielding, a load independent push-pull (differential) Class EF inverter, and a full-wave voltage-tripler Class D rectifier, a DC-DC efficiency of 84 % was achieved by the IPT system.

ACKNOWLEDGEMENT

The authors would like to acknowledge the following funding sources: EPSRC Quietening ultra-low-loss SiC & GaN waveforms, grant ref: EP/R029504/1; EPSRC Impact Acceleration Account - Imperial College London 2017, grant ref: EP/R511547/1; EPSRC Converter Architectures, grant ref: EP/R004137/1.

REFERENCES

[1] C. H. Kwan, J. M. Arteaga, D. C. Yates, and P. D. Mitcheson, "Design and construction of a 100 w wireless charger for an e-scooter at 6.78 mhz," in *2019 IEEE PELS Workshop on Emerging Technologies: Wireless Power Transfer (WoW)*, 2019, pp. 186–190.

[2] "Govecs GO! S2.4 – Electric Moped Scooter 2019," https://www.e-scooter.co/govecs-go-s2-4/, January 2019.

[3] R. E. Zulinski and K. J. Grady, "Load-independent Class E power inverters. i. theoretical development," *IEEE Transactions on Circuits and Systems*, vol. 37, no. 8, pp. 1010–1018, Aug 1990.

[4] S. Aldhaher, D. C. Yates, and P. D. Mitcheson, "Load-independent Class E/EF inverters and rectifiers for MHz-switching applications," *IEEE Transactions on Power Electronics*, vol. 33, no. 10, pp. 8270–8287, Oct 2018.

[5] J. M. Arteaga, S. Aldhaher, G. Kkelis, C. Kwan, D. C. Yates, and P. D. Mitcheson, "Dynamic capabilities of multi-MHz inductive power transfer systems demonstrated with batteryless drones," *IEEE Transactions on Power Electronics*, vol. 34, no. 6, pp. 5093–5104, June 2019.

[6] M. M. Weiner, "Analysis of cockcroft-walton voltage multipliers with an arbitrary number of stages," *Review of Scientific Instruments*, vol. 40, no. 2, pp. 330–333, 1969.

[7] S. Park, J. Yang, and J. Rivas-Davila, "A hybrid cockcroft–walton/dickson multiplier for high voltage generation," *IEEE Transactions on Power Electronics*, vol. 35, no. 3, pp. 2714–2723, 2020.